Time Fluctuations and Imaging in the SERS Spectra of Fungal Hypha Grown on Nanostructured Substrates

Adriana Szeghalmi,[†] Susan Kaminskyj,[‡] Petra Rösch,[§] Jürgen Popp,[§] and Kathleen M. Gough*,[†]

Department of Chemistry, University of Manitoba, Winnipeg, MB R3T 2N2, Canada, Department of Biology, University of Saskatchewan, Saskatoon, SK S7N 5E2, Canada, and Institut für Physikalische Chemie, Friedrich-Schiller-Universität Jena, 07743, Germany

Received: July 11, 2007; In Final Form: August 31, 2007

Surface-enhanced Raman scattering (SERS) spectroscopy is an emerging technique in biomolecular analysis that can have a tremendous impact in the life sciences. We report on the SERS imaging of fungal hyphae grown on nanostructured SERS active substrates engineered using semiconductor technologies. Time fluctuations in the intensity and band position in the SERS spectra measured on the same sample position with 1 s integration time have been observed indicating that the SERS signal arises from a limited number of molecules and that possibly single components are being detected.

1. Introduction

With surface-enhanced Raman scattering (SERS), the Raman cross section of molecules adsorbed onto silver or gold nanoparticles is increased by several to many orders of magnitude (up to 10^{15}).[1] This increase suggests the attractive possibility of using SERS spectroscopy to image biological samples, combining high spatial resolution with short integration time; however, several challenges remain. In general, only compounds within 10 nm from the active substrate will experience the SERS enhancement. Technical considerations include (1) production of well-defined, reproducible SERS substrates, (2) chemical heterogeneity of biological samples, which produce complex SERS spectra, and (3) preferential adsorption of components onto the SERS substrate, leading to nonrepresentative spectra.

Consistent with the expected increase in scattering intensity, several groups have reported single molecule detection using SERS spectroscopy.[1−17] This conclusion is based on the observation of time-dependent intensity fluctuations (blinking) in the SERS spectra recorded from molecules adsorbed on nanoparticles. The rationale is that many molecules would not move or change their orientation at the same time in a synchronized manner. The possibility of single molecule detection presents additional applications for SERS imaging.

Here, we report a SERS study of dried fungal hyphae grown on commercially available nanostructured gold-coated substrates. These are produced using nanofabrication techniques and offer a well-characterized and reproducible substrate possibly adequate for in situ or in vivo imaging studies. The SERS spectral maps of the fungal system are correlated with Raman maps and scanning electron microscopy (SEM) images. High-quality SERS spectra have been obtained with as little as 1 s integration time. In the SERS maps, signals detected a few micrometers from the fungal hyphae are attributed to secreted extracellular matrix compounds, showing the high sensitivity of the SERS substrates. Intriguingly, time fluctuations in the SERS spectra recorded at positions on the sample with very large enhancement have been observed. Several bands were present for up to 1 min while others disappeared within seconds. The time scale of these surface dynamics indicates a thermally activated diffusion of various fungal components and demonstrate the dramatic SERS enhancement enabled by such nanostructured substrates.

2. Methods

Aspergillus nidulans strain A28 (*biA1*, *pabaA6*, *veA1*; www.fgsc.net) was grown on a Klarite SERS substrate (Mesophotonics Ltd.) essentially as described previously.[18] Briefly, a block of sterile potato dextrose agar (Difco), pH 6.5, was lightly coated on one side with fresh *A. nidulans* spores, placed on one edge of the Klarite SERS substrate, and incubated inverted (the agar retained by surface tension) in a moist chamber at 100% relative humidity for 24 h at 28 °C. Hyphae grew across the substrate, drawing nutrients from the agar. The SERS substrate consists of a gold-coated regular nanotextured array bordered by a smooth gold-coated surface, and thus hyphae also grew across regions suitable for analysis by ordinary Raman scattering. Following growth, the slide assembly was placed on a clean metal surface at −80 °C (inoculated side facing up) until frozen and then was lyophilized to dryness in a Labconco Freezone 6.

Raman and SERS maps of *A. nidulans* grown over Klarite SERS substrates were collected with a micro-Raman instrument (HR LabRam invers, Jobin-Yvon-Horiba). The 632.8 nm excitation wavelength of a HeNe laser, output ∼ 4 mW, was focused onto the sample with a Leica PLFluoar 100× objective (N.A. 0.75). The spectrometer was equipped with a 300 lines/mm grating, and the scattered Raman light was detected with a cooled CCD. Maps were created by raster scans over single fungal hyphae using a computer-controlled *x*/*y* motorized stage (Mertzhäuser) and 1 μm step size. Initially, fungal hyphae were mapped to locate regions with high SERS enhancement compared to Raman scattering maps. Subsequently, several time-lapse series, consisting of 100−300 SERS spectra with 1−10 s

* Author to whom correspondence should be addressed. Phone: (204) 474-6262; fax: (204) 474-7608; e-mail: kmgough@ms.umanitoba.ca.
[†] University of Manitoba.
[‡] University of Saskatchewan.
[§] Friedrich-Schiller-Universität.

10.1021/jp075422a CCC: $37.00
Published on Web 10/18/2007

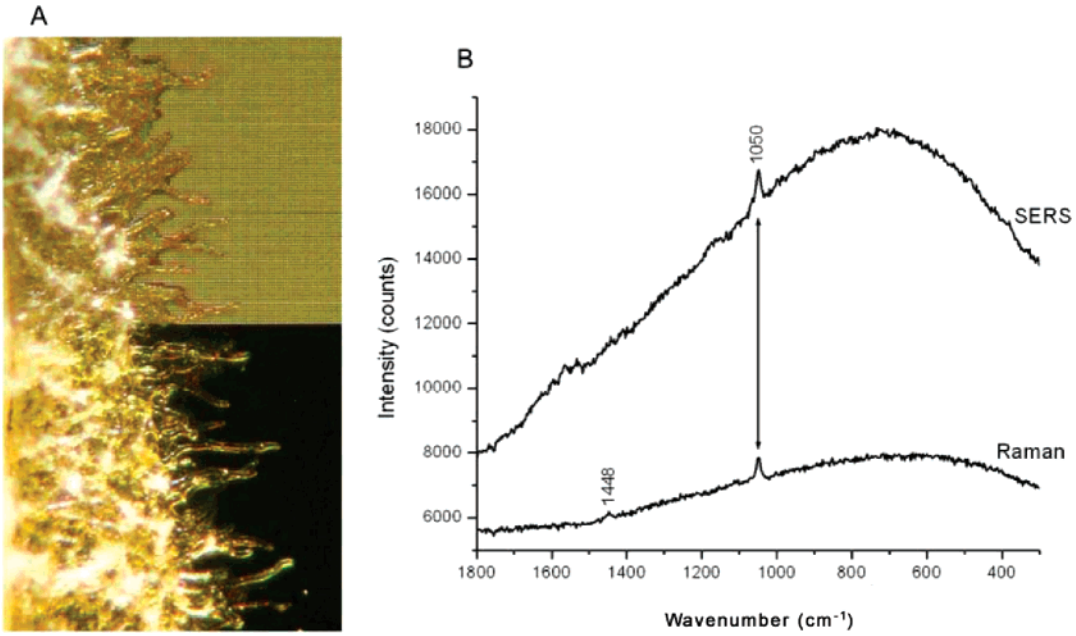

Figure 1. (A) Photoimage of the Klarite substrate showing the SERS-active pattern grid area (top half) and the smooth border (lower half). The fungi grown on the nanostructured region show no remarkable difference from those on the smooth area. (B) Representative Raman and SERS spectra of *A. nidulans*.

integration time/spectrum, were measured on several individual "hot spots" (see below). The total measurement time for a time series of 300 spectra with 1 s/spectrum was 350 s. Following data collection, the hyphae were visualized with SEM (Cambridge Stereoscan 120 scanning electron microscope).

The majority of the spectra presented show the raw data. In some SERS spectra, the strong, regular background was subtracted with a sixth-order polynomial function, using the LabSpec software available with the instrumentation.

3. Results and Discussion

3.1. Sample Morphology and Condition. The gold-coated SERS substrate consists of a patterned region ~4 × 4 mm in area, surrounded by a smooth border (Figure 1A). The hyphae grew over the slide without contaminating the SERS substrate with nutrients from the agar. In regions very close to the agar block, a deposit extended outward with the hyphae, indicating that the agar/nutrient mixture had possibly flowed along the surface by capillary action; however, this behavior was not observed further along the growing hyphae to where data were recorded. Some contamination from the humid chamber could not be excluded as a possibility. Survey spectra of the peripheral unused regions on the SERS substrate yielded minimal contamination signals (see section 3.5 below).

3.2. Comparison of Raman and SERS Maps. Our first concern was to determine whether the SERS substrate would give signal enhancement compared to Raman spectroscopy. Since the fungal growth extended over both the smooth border and the patterned SERS grid (Figure 1A), signals could be compared for hyphae grown under essentially identical conditions. Spectral scans from 200 cm^{-1} to 1800 cm^{-1} for hyphae on smooth (Raman) and patterned grid (SERS) surfaces are compared in Figure 1B. Spectra were acquired from 633 nm excitation wavelength with 180 s integration time for Raman and 10 s for SERS. A strong peak at 1050 cm^{-1} shows an identical vibrational signature in both Raman and SERS spectra. The Raman spectra also displayed a very weak peak at 1448 cm^{-1}, but this was not seen on the SERS substrate. The background in the SERS spectra is somewhat higher despite the much shorter integration time, as it is due not only to fluorescence but also to the emission continuum typically observed in SERS.[19]

A hypha growing well away from the agar block on the smooth region was selected for Raman mapping; data were collected at 180 s/spectrum, with a spatial resolution of 1 μm (Figure 2A, SEM image; 2B, Raman microscope video image). The map spectra were processed to give a false color image that displays the intensity of the peak at 1050 cm^{-1}; maximum intensity corresponds to about 500 counts/180 s (Figure 2C). The signal intensity is essentially restricted to the hypha and is absent in the rest of the map. The peak at 1050 cm^{-1} was the only strong band in all the normal Raman spectra.

A comparable hypha grown on the SERS surface (Figure 2D, SEM) was mapped at 10 s/spectrum also at a spatial resolution of 1 μm. The area corresponding to the mapped image is outlined by the green box (Figure 2E) and again (Figure 2F) with the hypha outlined in yellow as the profile is less obvious against the SERS grid. The yellow hyphal profile has been copied onto the false-color spectral map image (Figure 2F) again processed to display the intensity at 1050 cm^{-1}. The maximum intensity on the SERS map is about 800 counts/10 s for a signal enhancement factor of about 30 relative to the Raman map.

A distinctly different intensity pattern is seen for the SERS map (Figure 2F) compared to the smooth surface Raman map (Figure 2C). First, in the SERS map, the strongest intensity is recorded at points around the hypha, although it is present to some extent in all pixels on the hypha. Second, the pattern of intensity distribution mirrors the SERS grid template. These observations may be caused by restrictive "first-layer SERS enhancement" with the probe being in direct contact or in close vicinity with the substrate[20] and may be due to pooling of secreted extracellular material along the grid pattern. We next consider these factors in more detail.

3.3. Distribution of 1050 cm^{-1} Signature. The results in section 3.2 raise the intriguing question of why the 1050 cm^{-1} signal extends around the hypha in the SERS spectra but not in

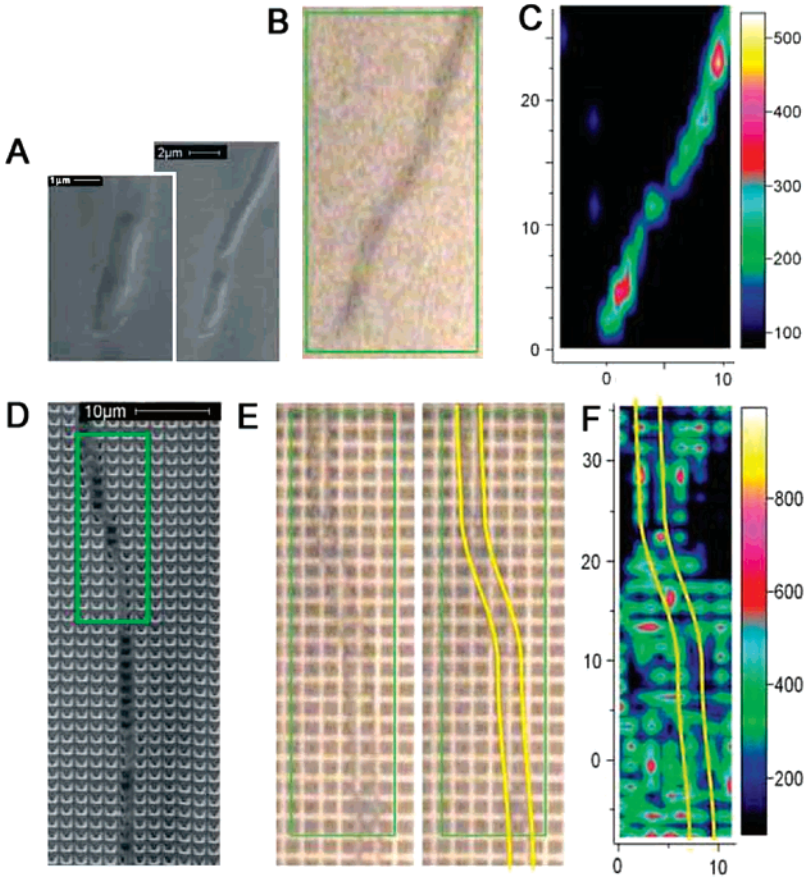

Figure 2. SEM (A, D) and photo images (B, E) of fungi grown over smooth gold surface and SERS active region, respectively. Raman (C) and SERS (F) spectral maps processed for the area of the band at 1050 cm^{-1} for the regions outlined in the photoimages B and E. Spectral maps were measured at 633 nm excitation with 180 s integration time for Raman and 10 s for SERS. Color bars show correspondence between band area and processed map colors.

the Raman map. Line maps were recorded along several hyphae beginning at a distance of ~30 μm out from the tip and continuing along the hypha for another ~30 μm (Figure 3). The band at 1050 cm^{-1} was observed only within 3−5 μm from the tip in the SERS map and thus must be associated only with the growing hypha.

During growth, fungi secrete materials with diverse functions; some extracellular matrix (ECM) components act as adhesives,[21,22] and others play roles in cell wall formation. Hydrolytic enzymes (proteases, lipases, glycosidases) are secreted to break down insoluble substrates; organic acids, some of which scavenge Fe and P, are released and resorbed.[23] The SEM images of hyphae grown over the smooth gold surface show a halo around the fungal wall indicating secreted material[21] (see also Figure 2A). Some of these materials may have spread over the SERS substrate around the hypha during growth. Capillary effects would facilitate the flow of any fluid material into the pits of the SERS substrate.

A further explanation for the observed SERS intensity pattern relates to the localized plasmon characteristics of the SERS substrates. The role of the localized surface plasmons in the electromagnetic enhancement of the Raman scattering of molecules in the vicinity of metal nanoparticles is well established.[24−28] Periodic nanotexturing of metal surfaces can lead to the formation of surface plasmons and, hence, the growing interest in engineering SERS substrates using semiconductor technologies. Photon scanning tunneling microscopy demonstrated that surface plasmons are bound to the metal surface[25] of periodic metal nanostructures. Through theoretical modeling of the Klarite substrate's structural parameters, Netti et al. predicted a localized electromagnetic field confined at the edges and in the pit.[28]

Surface plasmons are ideal for transducing incident electromagnetic radiation into molecules, enhancing the Raman scattering by many orders of magnitude. The incident light excites localized surface plasmons, which excite molecular dipoles that then lose packets of energy to phonon vibrations.[28] Given that the mapping coordinates are not precisely aligned with the SERS grid and that the laser focus spot is on the order of the pit dimensions (~1 μm), it is reasonable to assume that the laser will not perfectly excite all localized surface plasmons at each step. The band at 1050 cm^{-1} does not vanish, but its intensity is reduced in a pattern that follows the nanotexture of the pyramidal pits. Further research is required to determine the cause of this peculiar pattern of intensity distribution, possibly by SERS mapping at higher spatial resolution.

These results demonstrate that the SERS substrates are promising for spectroscopic imaging. The same signature (1050 cm^{-1}) is obtained in both the Raman and SERS spectra, but the data collection is 30× faster for the SERS; larger areas may be scanned much more rapidly when a known target peak is available.

3.4. Time-Lapse Spectra at a Single Point. Interestingly, although ~75% of the fungal SERS spectra had only one peak, namely, at 1050 cm^{-1}, ~5% of the spectra had numerous strong bands. About 7% of the spectra from the fungal SERS map showed clear carbon bands (see section 3.5), whereas about 13% had no features (black region in the spectral map, Figure 2F).

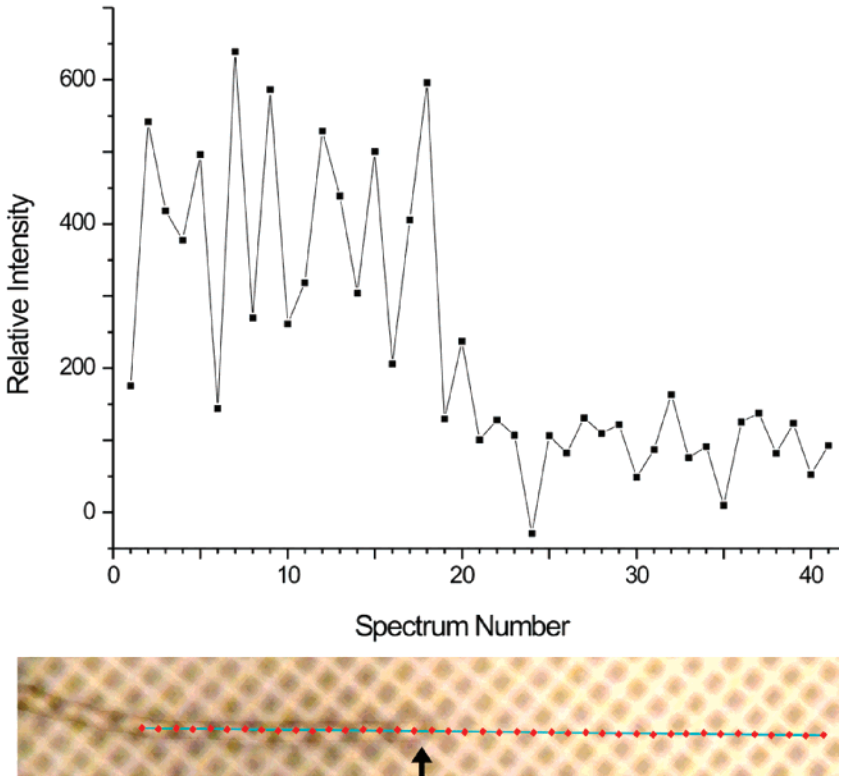

Figure 3. Representative line map of a fungal hypha with the intensity plot of the band at 1050 cm^{-1}. The red points on the hypha image (bottom) indicate the measurement position and correlate with the squares in the intensity distribution profile (top). The single-headed arrow indicates the approximate tip of the fungal hypha between pixels 17 and 18.

In the spectra with many features, the SERS intensities of several bands greatly exceed the intensity of the band at 1050 cm^{-1}. Some of the spots on the SERS substrate map where the enhancement was strong were reexamined. SERS spectra were recorded over a time series of 300−450 s with 1−5 s integration time per spectrum. Figure 4 presents such a time series plot of 300 spectra with an integration time of 1 s/spectrum (actual measurement time 350 s because of computer readout). No background subtraction or smoothing procedures were applied to these spectra.

Strong peak intensity fluctuations for several bands are observed over time, but the standard deviation of the SERS intensity of the band at 1050 cm^{-1} over time is minimal (marked with an arrow in Figure 4). In the 300 spectra obtained on the same spot, the temporal standard deviation of the peak intensity at 1050 cm^{-1} and of the background estimated at 300 and 1800 cm^{-1} was less than 4%. There was no correlation between SERS fluctuations and background intensity. Netti et al.[28] analyzed the Klarite SERS substrates and indicated good spatial reproducibility with a spatial standard deviation of 10% for the peak intensity of reference materials. Since the intensity of the band at 1050 cm^{-1} and the background shape remain constant, we conclude that photodecomposition during measurement and laser illumination is minimal and that the fluctuations in the other peaks must arise from some other cause.

The peak intensities at 611 and 1419 cm^{-1} are plotted as a function of time in Figure 5 to illustrate the time scale of the changes in individual peaks in the SERS spectra. The background has been subtracted for clarity. The peaks at 611 and 1419 cm^{-1} appear in consecutive spectra recorded over time intervals of up to 50−60 s. These appearances are not related; some coincide, others do not. The insert shows the intensity of the peak at 1419 cm^{-1} for the time interval from ∼300 to 310 s when the SERS enhancement is particularly high. The insert demonstrates that three short, "blinking" periods for the SERS enhancement have occurred in less than 10 s.

A closer examination of the spectra recorded between 301 and 311 s (Figure 6A) reveals short-time dynamics on the SERS substrate. The intensity of the 1419 cm^{-1} peak reaches ∼2000 counts for 2 s (at 302 and 303 s). In subsequent spectra, the peak is overlapped by a very strong band at 1410 cm^{-1}. The peak at 1339 cm^{-1} can be observed in four consecutive spectra, while the peak at 990 cm^{-1} exhibits strong enhancement only in 1 spectrum out of 10 (at 303 s) rapidly fading at 304−305 s and absent thereafter.

In contrast, the spectra shown in Figure 6B (time interval from 257 to 267 s) and in Figure 6C (from 175 to 185 s) reveal several bands that persist for longer periods. In particular, the peaks at 1294, 1124, 976, 882, and 611 cm^{-1} can be identified in all spectra of Figure 6B. The peaks at 1294 and 1124 cm^{-1} are also present in most of the spectra in Figure 6C, which also shows consistent bands at 1419, 1391, and 606 cm^{-1}. Hence, recording hundreds of SERS spectra with 1 s integration time made possible the simultaneous observation of both short-time (∼1 s) and relatively long-time (∼1 min) molecular dynamics on the gold substrate.

Several SERS studies have attributed time fluctuations in SERS spectra to single molecule detection.[1−17] Most of these studies analyzed SERS active nanoparticles with a statistically small number of analyte molecules per particle. Despite the increasing amount of research to understand the physical or chemical origin of the blinking effect, there is still considerable controversy. Fluctuation in the enhanced electromagnetic field intensity in the vicinity of the nanoparticles (photochemical contribution) has been proposed.[1,2] Other studies[4,12−17] attributed the SERS intensity fluctuations to the nanoscale motions of the

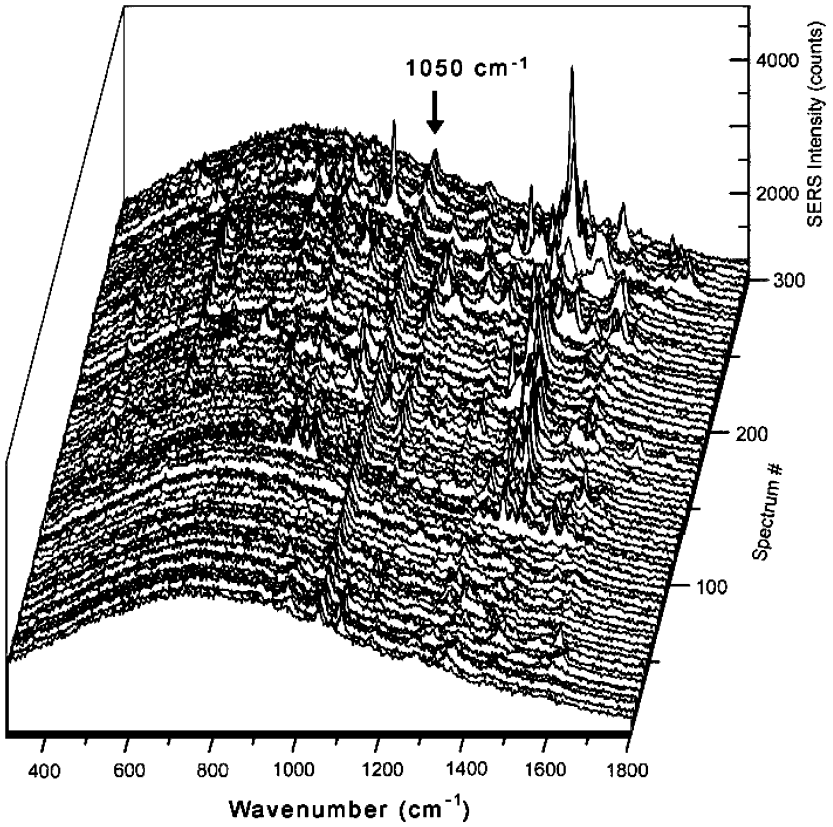

Figure 4. Time-dependent SERS spectra of *A. nidulans* recorded with 1 s integration time showing every fifth spectrum. The background has not been subtracted. Total measurement time was ~350 s, and a total of 300 spectra were recorded.

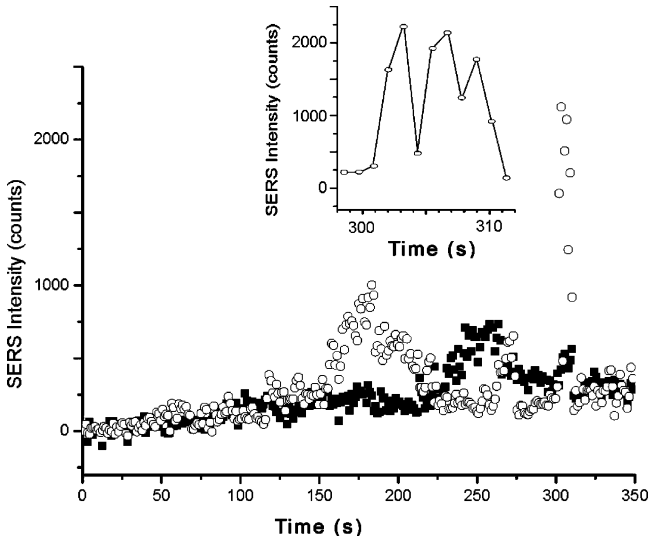

Figure 5. Plot of the SERS intensity of the spectra in Figure 4 for the peak positions at 611 (■) and 1419 cm^{-1} (○) as function of time. The same background line has been subtracted from all 300 spectra. Insert shows an enlargement of the peak intensity at 1419 cm^{-1} from ~300 to 310 s with rapid intensity fluctuation. The insert shows the region from 300 to 310 s with the time scale expanded.

molecule in and out of the hot spot. Temperature-dependent studies[13,17] have demonstrated that the blinking is thermally activated, ascribed most probably to thermally-facilitated diffusion of the adsorbed molecule or changes in the orientation of the molecule on the substrate during diffusion.

While most studies have focused on the detection of single molecules for ultralow analyte concentration, single molecule detection in a mixture of two dyes by SERS has recently been reported.[29] The Bi-Analyte SERS (BiASERS)[29] study found several nanosilver clusters where only one compound was detected despite the statistical probability of there being 500 molecules of each dye per cluster. Unfortunately, no time-dependent measurements were performed in the BiASERS study.

Chemically, the fungal hypha is an extremely complex system and comparison with such a Bi-Analyte system is a gross approximation. Moreover, it seems unlikely that the Klarite SERS substrates have single molecule detection capacity. Theoretically, such single molecule detection requires enhancement factors of over $10^{10}-10^{14}$, and it is assumed that the Klarite substrates[28] provide a maximum SERS enhancement factor of only $10^{5}-10^{6}$. In contrast, recent theoretical calculations[30] based on Mie theory predicted that arrays of metal nanoshell dimers could yield local electromagnetic enhancement of $10^{13}-10^{14}$. Zhao el al. attributed the extraordinarily high theoretical enhancement to a long-range collective photonic effect constructively superposed onto the enhancement associated with localized surface plasmons.[30] The short-time fluctuations in our SERS spectra indicate that the signal is due at most to a limited number of molecules and are the first experimental evidence that such nanostructured substrates may have single molecule sensitivity.

The time-dependent spectra in this study also demonstrate that several different compounds are experiencing the SERS enhancement concurrently, since some peaks are present for several seconds up to 1 min (see Figures 4−6) while others appear and disappear in shorter intervals (see Figure 6). This is actually strong evidence that a small number of molecules are being detected using the Klarite substrates. The degree of mobility of some fungal components is presumably limited by

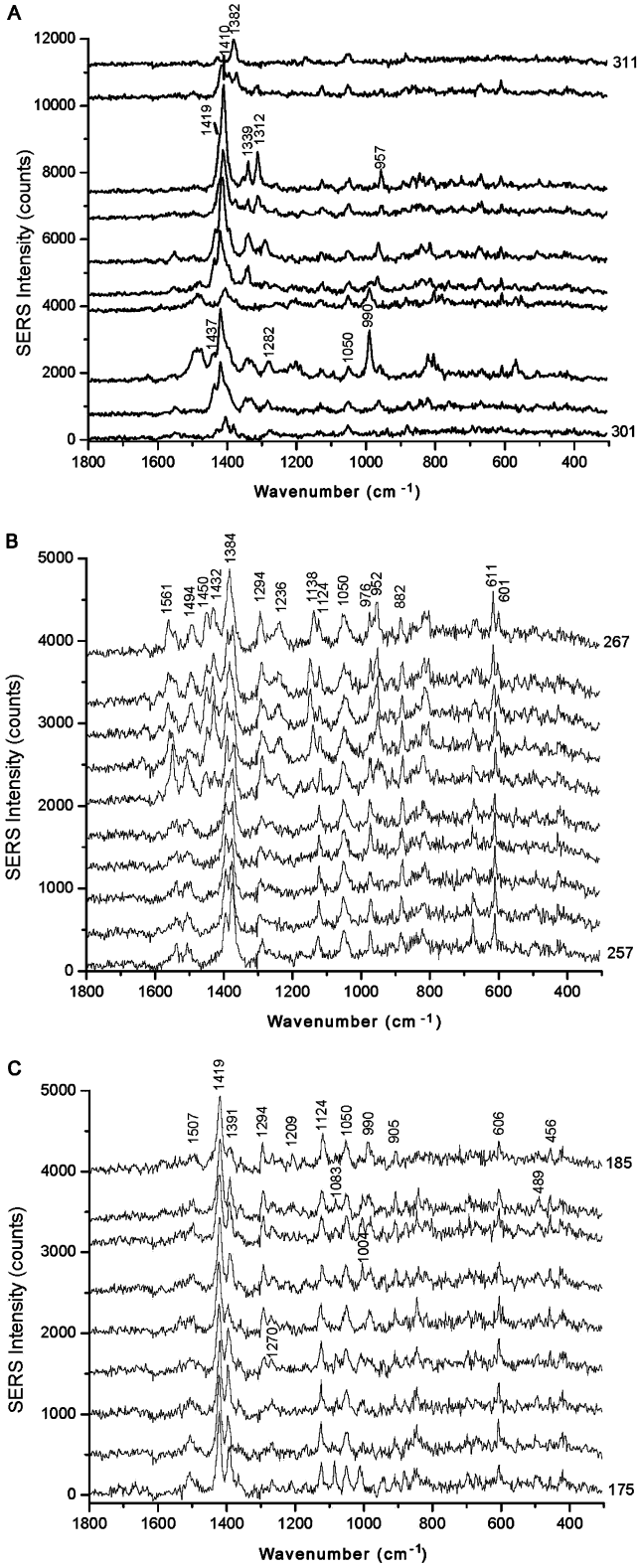

Figure 6. Selected SERS spectra recorded between time intervals as indicated (A from 301 to 311 s, B from 257 to 267 s, and C from 175 to 185 s). 6A shows strong intensity fluctuations while in 6B and 6C most bands have comparable intensities over several seconds. Integration time 1 s; background has been subtracted. Spectra are plotted on the same scale as indicated and are offset for clarity.

intermolecular interactions with other compounds within the structural matrix. While some compounds are more tightly bound to the substrate and have lower mobility, eventually another component could undergo thermal diffusion into the hot spot and could experience strong surface enhancement for a short time. Changes in the orientation or conformational structure of some molecules (glycoproteins or polysaccharides) during diffusion are also likely to occur, and perhaps these contribute to the spectral fluctuations. It is not plausible that a high number of molecules would diffuse or change their orientation in a synchronized fashion. In addition, the confined local electromagnetic field (about 10 nm) limits the number of molecules that may give rise to the dominant SERS signal.[10]

In some of the time-dependent studies,[5,13,17] the blinking of gold colloids was reported on the time scale of milliseconds. However, the studies of Etchegoin et al.[9] and Krug et al.[2] were able to differentiate between resonantly and nonresonantly excited molecules adsorbed onto nanoparticles. They showed that the rate and intensity of time fluctuations depend on the excitation wavelength and analyte type. The present study using Klarite substrates also differentiates between molecules with various adsorption/desorption rates. The SERS signal fluctuates on the time scale of seconds which is more typical of thermal processes rather than instantaneous photochemical effects and changes in the local electromagnetic field.[9]

The BiASERS study[29] strongly indicated that the number of the hot spots is much larger than previously believed and that the determining factor for single molecule detection is the presence or absence of an analyte at the right position. Despite the intense work in this area, the present knowledge about SERS substrates is limited, and there are only a few time- and space-resolved studies. The present work employing Klarite SERS substrates also suggests that single molecule detection can be achieved and is possibly more common than currently expected.

3.5. Average of Time-Dependent SERS Spectra. Several studies report the presence of amorphous carbon on SERS substrates because of photodecomposition. Kudelski and Pettinger[4,12,15,16] showed that such carbon nanocrystalline clusters also exhibit narrow SERS bands with significant fluctuations in number, intensity, and wavenumber. However, when numerous (~40) SERS spectra with high fluctuations were averaged, the resulting spectrum corresponded to the Raman spectrum of amorphous carbon with broad bands at about 1350 and 1580 cm^{-1}.

The average spectra of several SERS time series recorded from the fungi with high-intensity fluctuations are presented in Figure 7. The strongest band appears at 1050 cm^{-1} since this peak is present in all spectra and its intensity adds up to the highest in the average spectrum. The average spectra are clearly not corresponding to amorphous carbon. Several bands can be identified in two or more average spectra. The bandwidth of the peaks is quite large. Small shifts in the peak position of vibrational modes have been observed in the time-lapse measurements and were also reported previously in time-dependent SERS studies;[13] thus, the band broadening may be due to small changes in the molecular orientation on the substrate during the measurement (see vibrational analysis below).

We have recorded SERS maps on regions of the gold substrate where no fungal grew (~2 mm from the fungi tips). Only 5 out of 121 SERS spectra from bare substrate showed characteristic broad bands because of amorphous carbon, corresponding to three carbon clusters on an 11 × 11 μm^2 region. Three of these spectra were due to a single cluster spread across three contiguous pixels. The spectra were recorded at 1 μm spatial resolution with 1 s integration time. One SERS spectrum from the substrate shows an intense band at 1166 cm^{-1}. The presence of the impurities can be due to contamina-

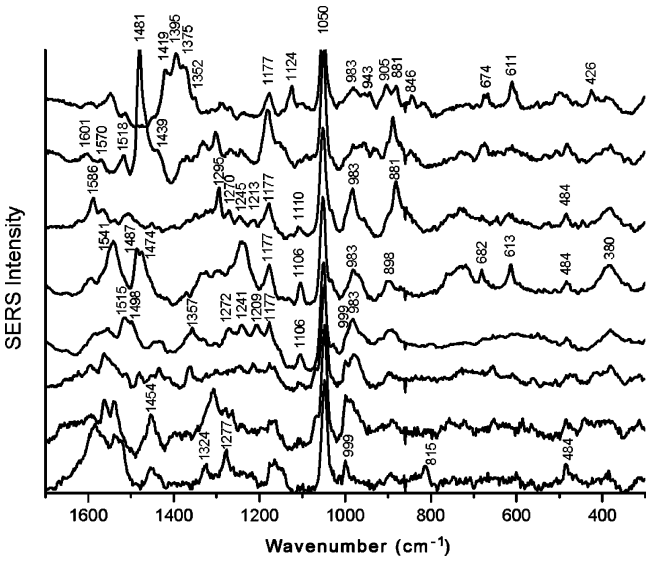

Figure 7. Average spectra of SERS time-dependent measurements recorded on hot spots with strong intensity fluctuations. A total of 90−300 SERS spectra obtained with 1−5 s integration time/spectrum were averaged.

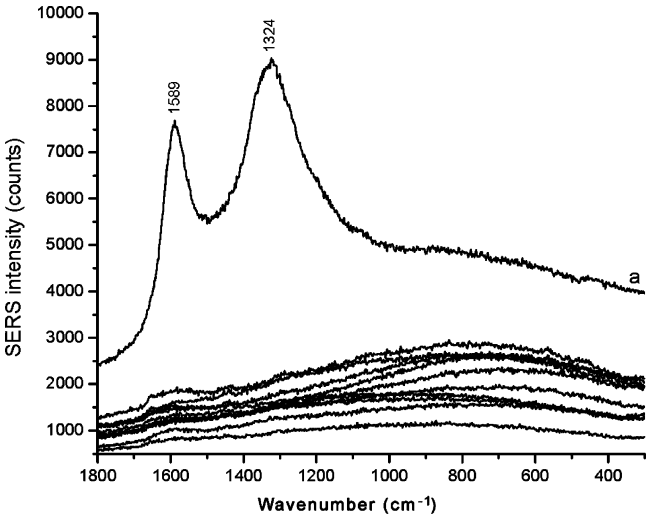

Figure 8. Selected SERS spectra recorded from gold substrate in absence of fungi (∼1−2 mm from fungal tips). Integration time 1 s; spectra recorded in a row with 1 μm spatial resolution. Spectrum a shows characteristic amorphous carbon bands.

tions from air during storage or during the incubation time (24 h) in a humid environment. We estimate that approximately 5% of the substrate is contaminated in this way. Characteristic amorphous carbon bands were identified in about 7% of the spectra in the SERS map outlined in Figure 2E (see section 3.4). Hence, the contamination on the hypha is minor and is comparable to the blank reference regions on the substrate.

Figure 8 presents selected unprocessed SERS spectra from the gold substrate far (∼2 mm) from the fungi. The spectrum of the amorphous carbon cluster shows no narrow lines (halfwidth < 20 cm^{-1}) or any shoulders as reported in previous SERS studies of nanocrystalline carbon. The SERS spectra in Figure 8 also show that the background of the SERS substrate itself is low; the background spatial variation is insignificant and there are no Raman bands because of the SERS substrate. From these results, we conclude that the fluctuations observed in the SERS spectra of the fungi are not due to carbon decomposition or to other substrate-related artifacts.

3.6. Vibrational Assignment. The ultimate goals of this ongoing study[18] are to understand the chemical changes that occur during maturation of the fungal hyphae and how genetic mutations and environmental conditions affect organism phenotype. This is a very difficult objective despite the fact that Raman and SERS spectroscopy has been extensively applied to the study of biological compounds, bacteria, fungi, plant, and tissue specimens.[20,31−45] However, the relative intensities and wavenumbers of the bands in the Raman and SERS spectra of a molecule are not identical. Through the interaction of the molecule with the metal substrate, Raman forbidden modes can become allowed in the SERS spectra. Further, according to SERS selection rules,[24] vibrations with polarizability components perpendicular to the metal substrate are enhanced and will give rise to strong SERS bands. Hence, orientation of the molecule onto the substrate affects the SERS spectrum. Variation of concentration and pH can also induce drastic changes in the SERS spectra.[46,47]

In general, cell or tissue specimens give rise to Raman spectra[31−38] characterized by broad bands around 1650 cm^{-1}, the amide I protein C═O stretching vibration; 1575 cm^{-1} because of DNA and RNA components; 1440−1460 cm^{-1}, the methyl and methlyene deformation modes of lipids, polysaccharides, and proteins; around 1285−1350 cm^{-1}, the protein amide III deformation of N−H and C−H; and 1000−1200 cm^{-1} corresponding to C−C and C−O stretching modes of lipids and polysaccharides. Only a few vibrational modes of biomacromolecules give rise to sharp, signature peaks in their Raman spectra, such as the phenylalanine ring breathing mode around 1004 cm^{-1}. Despite the biochemical complexity of biological specimens, their vibrational spectra have been correlated in some instances with specific compounds. The Raman spectra of *Lactarius* spores could be correlated with triolein as a major lipid component,[31] mitochondria could be correlated with phosphatidylcholine,[32] calcium dipicolinate has been detected in bacterial *Bacillus* spores,[38] and the creatine vibrational signature has been identified in the spectra of brain tissue sections.[34]

The difficulty of interpreting the Raman spectra of biological samples lies primarily in the fact that all biochemical constituents are detected simultaneously, resulting in broad bands because of overlap. Complex fitting procedures have been attempted to discriminate between cellular components,[33] but their success is limited. Through the enormous enhancement of the Raman signal via surface plasmons, the SERS spectra of biological specimens correspond to signal from only a small fraction of the tissue constituents or even individual biochemical components. In addition, the single molecule SERS spectra are characterized by narrower bandwidths (11 cm^{-1}) ca. $^1/_2$ the normal width for samples at higher concentrations.[13] Hence, the overlap between numerous peaks is reduced and the resulting SERS spectra generally show sharp bands[39−45] (see also Figures 4 and 6).

We have recorded several hundreds of SERS spectra with short (1−5 s) integration times providing numerous spectra with distinctive vibrational chemical signatures. Individual analysis of each spectrum is not the objective of the present publication. A tentative vibrational assignment of some representative bands is given in Table 1. An exact vibrational assignment and possibly identification of individual components requires considerable further experiments. Candidate compounds include not only the

TABLE 1: Tentative Vibrational Assignment of the Most Prominent SERS Peaks Observed in the Time-Dependent Measurements Recorded at Locations on the Substrate with Extraordinary Enhancement

wavenumber/cm^{-1}	tentative assignment
426, 456	CCC, CC═O deformation
484, 489	CCC deformation
601, 611, 613	COO^- deformation
815	phosphate
881, 882, 898	νC−C, saccharides
905	lipids
943, 952, 957, 976	νC−C, νC−C−N, νC−COO^- proteins, saccharides, lipids
983, 990	νC−C sugar, lipid
999	CH_2 rocking
1004	phenyl ring breathing mode
1050	νC−O, νC−C sugar, lipid, C−H deformation
1106, 1110, 1124	νC−O, νC−C, CC−H deformation
1124, 1138, 1177	νC−O, νC−C sugar, lipid
1209, 1213, 1236	ring stretching, CC−H deformation
1241, 1245	amide III
1270, 1272, 1277	CH_2 wagging
1294, 1295, 1312	CH_2 wagging
1352, 1357	CH_3 deformation
1375, 1384, 1395	CH_2 scissoring
1419	$\nu_{sym}COO^-$
1432, 1450, 1454	CH_2, CH_3 deformation
1474, 1487, 1494, 1498	CH_3 deformation
1515, 1518	DNA
1541, 1561, 1570, 1586	$\nu_{asym}COO^-$
1601	νC═C

external hyphae wall molecules but are also the secreted extracellular matrix materials.

Future research should be directed toward both biomacromolecules and low molecular weight compounds adsorbed onto these nanostructured SERS substrates possibly combined with other high-sensitivity techniques such as mass spectrometry. Additionally, further research is necessary to thoroughly characterize these substrates. Elucidation of the observed time fluctuations and localized SERS enhancement could help in the development of improved SERS substrates, which is the goal of several research initiatives.[48−51]

Conclusions

Nanostructured SERS substrates have been investigated for imaging applications at high-spatial resolution (1 μm). An advantage of such materials engineered on the basis of photonic crystal and semiconductor technologies over previously developed SERS active nanoparticles or electrochemically roughened SERS substrates is their high reproducibility. The SERS active region permits considerable reduction in the measurement time necessary for a good signal-to-noise ratio compared to Raman spectra on the smooth region of the substrate. Therefore, gold-coated nanostructured materials as SERS substrates are promising in the analysis or screening of large sample areas. The high sensitivity of these SERS substrates is also indicated by the strong signal detected around the hyphal wall because of the extracellular matrix components excreted during growth. An intensity pattern superimposed onto the nanostructure of the substrate has been observed, which greatly obstructs quantitative measurements at high-spatial resolution. This intensity pattern is possibly associated with the localized nature of the surface plasmons.

Remarkable time fluctuations in consecutive SERS spectra recorded on the same sample position with 1 s integration time have been observed. Several peaks could be detected in spectra for up to 1 min, while other bands were observed only for seconds. Some of the peak intensities and the background shape are constant over time; therefore, photochemical decomposition due to laser illumination is negligible. Some bands show up with strong intensity in a few spectra in the time-lapse measurements, concomitantly with other bands which are present in consecutive spectra. Thus, the SERS signal at such highly active positions on the substrate is due to a limited number of molecules and possibly to single molecule detection. The time fluctuations are attributed to a thermally activated diffusion of some fungal components into the SERS active spot. Tailored nanostructured materials for SERS spectroscopy offer very rich chemical information in biomolecular studies and are promising substrates in biosciences.

Acknowledgment. The authors thank NSERC Canada and CIHR for financial support. A.S. thanks the CIHR ITMHRT for a postdoctoral fellowship.

References and Notes

(1) Kneipp, K.; Wang, Y.; Kneipp, H.; Perelman, L. T.; Itzak, I.; Dasari, R. R.; Feld, M. S. *Phys. Rev. Lett.* **1997**, *78*, 1667.
(2) Krug, J. T.; Wang, G. D.; Emory, S. R.; Nie, S. *J. Am. Chem. Soc.* **1999**, *121*, 9208.
(3) Xu, H.; Bjerneld, E. J.; Käll, M.; Börjensson, L. *Phys. Rev. Lett.* **1999**, *83*, 4357.
(4) Kudelskj, A.; Pettinger, B. *Chem. Phys. Lett.* **2000**, *321*, 356.
(5) Moyer, P. J.; Schmidt, J.; Eng, L. M.; Meixner, A. J. *J. Am. Chem. Soc.* **2000**, *122*, 5409.
(6) Michaels, A. M.; Nirmal, M.; Brus, L. E. *J. Am. Chem. Soc.* **1999**, *121*, 9932.
(7) Michaels, A. M.; Jiang, J.; Brus, L. *J. Phys. Chem. B* **2000**, *104*, 11965.
(8) Otto, A. *J. Raman Spectrosc.* **2002**, *33*, 593.
(9) Etchegoin, P.; Liem, H.; Maher, R. C.; Cohen, L. F.; Brown, R. J. C.; Hartigan, H.; Milton, M. J. T.; Gallop, J. C. *Chem. Phys. Lett.* **2002**, *366*, 115.
(10) Suh, Y. D.; Schenter, G. K.; Zhu, L.; Lu, P. *Ultramicroscopy* **2003**, *97*, 89.
(11) Etchegoin, P.; Liem, H.; Maher, R. C.; Cohen, L. F.; Brown, R. J. C.; Milton, M. J. T.; Gallop, J. C. *Chem. Phys. Lett.* **2003**, *367*, 223.
(12) Kudelskj, A.; Pettinger, B. *Chem. Phys. Lett.* **2004**, *383*, 76.
(13) Maruyama, Y.; Ishikawa, M.; Futamata, M. *J. Phys. Chem. B* **2004**, *108*, 673.
(14) Itoh, K.; Kudryashov, I.; Yamagata, J.; Nishizawa, T.; Fujii, M.; Osaka, N. *J. Phys. Chem. B* **2005**, *109*, 271.
(15) Kudelskj, A. *Chem. Phys. Lett.* **2006**, *427*, 206.
(16) Kudelskj, A. *J. Phys. Chem. B* **2006**, *110*, 12610.
(17) Emory, S. R.; Jensen, R. A.; Wenda, T.; Han, M.; Nie, S. *Faraday Discuss.* **2006**, *132*, 249.
(18) Szeghalmi, A.; Kaminskyj, S.; Gough, K. M. *Anal. Bioanal. Chem.* **2007**, *387*, 1779.
(19) Schatz, G. C. *Acc. Chem. Res.* **1984**, *17*, 370.
(20) Premasiri, W. R.; Moir, D. T.; Klempner, M. S.; Krieger, N.; Jones, G.; Ziegler, L. D. *J. Phys. Chem. B* **2005**, *109*, 312.
(21) Braun, E. J.; Howard, R. J. *Exp. Mycol.* **1994**, *18*, 211.
(22) Braun, E. J.; Howard, R. J. *Protoplasma* **1994**, *181*, 202.
(23) Deacon, J. W. *Modern Mycology*, 3rd ed.; Blackwell Science: Oxford, 1997.
(24) Suh, J. S.; Moskovits, M. *J. Am. Chem. Soc.* **1986**, *108*, 4711.
(25) Barnes, W. L.; Dereux, A.; Ebbesen, T. W. *Nature* **2003**, *424*, 824.
(26) Baumberg, J. J.; Kelf, T. A.; Sugawara, Y.; Cintra, S.; Abdelsalam, M. E.; Bartlett, P. N.; Russell, A. E. *Nano Lett.* **2005**, *5*, 2262.
(27) Kelf, T A.; Sugawara, Y.; Baumberg, J. J.; Abdelsalam, M. E.; Bartlett, P. N. *Phys. Rev. Lett.* **2005**, *95*, 116802-1.
(28) Netti, M. C.; Zoorob, M. E.; Charlton, M. D. B.; Ayliffe, P.; Mahnkopf, S.; Stopford, P.; Todd, K.; Lincoln, J. R.; Perney, N. M. B.; Baumberg, J. J. *Proc. SPIE* **2006**, *6093*, 95.
(29) Le Ru, E. C.; Meyer, M.; Etchegoin, P. G. *J. Phys. Chem. B* **2006**, *110*, 1944.
(30) Zhao, K.; Xu, H.; Gu, B.; Zhang, Z. *J. Chem. Phys.* **2006**, *125*, 0811021.
(31) De Gussem, K.; Vandenabeele, P.; Verbeken, A.; Moens, L. *Spectrochim. Acta, Part A* **2005**, *61*, 2896.
(32) Huang, Y. S.; Karashima, T.; Yamamoto, M.; Hamaguchi, H. *Biochemistry* **2005**, *44*, 10009.
(33) Short, K. W.; Carpenter, S.; Freyer, J. P.; Mourant, J. R. *Biophys. J.* **2005**, *88*, 4274.
(34) Gallant, M.; Rak, M.; Szeghalmi, A.; Del, Bigio, M.; Westaway, D.; Yang, J.; Julian, R.; Gough. K. M. *J. Biol. Chem.* **2006**, *281*, 5.

(35) Matthäus, C.; Boydston-White, S.; Milkovic, M.; Romeo, M.; Diem, M. *Appl. Spectrosc.* **2006**, *60*, 1.

(36) Maquelin, K.; Choo-Smith, L. P.; Endtz, H. P.; Bruining, H. A.; Puppels, G. J. *J. Clin. Microbiol.* **2002**, *40*, 594.

(37) Rösch, P.; Harz, M.; Peschke, K. D.; Ronneberger, O.; Burkhardt, H.; Popp, J. *Biopolymers* **2006**, *82*, 312.

(38) Chen, D.; Huang, S.; Li, Y. *Anal. Chem.* **2006**, *78*, 6936.

(39) Neugebauer, U.; Rösch, P.; Schmitt, M.; Popp, J.; Julien, C.; Rasmussen, A.; Budich, C.; Deckert, V. *Chem. Phys. Chem.* **2006**, *7*, 1428.

(40) Kneipp, J.; Kneipp, H.; McLaughlin, M.; Brown, D.; Kneipp, K. *Nano Lett.* **2006**, *6*, 2225.

(41) Kneipp, J.; Kneipp, H.; Rice, L. W.; Kneipp, K. *Anal. Chem.* **2005**, *77*, 2381.

(42) Sengupta, A.; Mujacic, M.; Davis, E. J. *Anal. Bioanal. Chem.* **2006**, *386*, 1379.

(43) Stewart, S.; Fredericks, P. M. *Spectrochim. Acta, Part A* **1999**, *55*, 1615.

(44) Jarvis, R. M.; Brooker, A.; Goodacre, R. *Faraday Discuss.* **2006**, *132*, 281.

(45) Jarvis, R. M.; Goodacre, R. *Anal. Chem.* **2004**, *76*, 40.

(46) Szeghalmi, A. V.; Leopold, L.; Pînzaru, S.; Chis, V.; Silaghi-Dumitrescu, I.; Schmitt, M.; Popp, J.; Kiefer, W. *Biopolymers* **2005**, *78*, 298.

(47) Szeghalmi, A. V.; Leopold, L.; Pînzaru, S.; Chis, V.; Silaghi-Dumitrescu, I.; Schmitt, M.; Popp, J.; Kiefer, W. *J. Mol. Struct.* **2005**, *735*−*736*, 103.

(48) Moger, J.; Cornes, N. L.; Vukusic, P. *Proc. SPIE.* **2007**, *6630*, 66330O.

(49) Goulet, P. J. G.; Aroca, R. F. *Anal. Chem.* **2007**, *79*, 2728.

(50) Zhang, W.; Yeo, B. S.; Schmid, T.; Zenobi, R. *J. Phys. Chem. C* **2007**, *111*, 1733.

(51) Braun, G.; Pavel, I.; Morrill, A. R.; Seferos, D. S.; Bazan, G. C.; Reich, N. O.; Moskovits, M. *J. Am. Chem. Soc.* **2007**, *129*, 7760.